Determining the clock frequency shift due to collisions in a 1-D optical lattice clock with ^{88}Sr

J.S.R. Vellore Winfred, Ch. Lisdat, T. Middelmann, F. Riehle and U. Sterr
Physikalisch-Technische Bundesanstalt
Bundesallee 100, 38116 Braunschweig
Germany
Email: raaj.vwjoseph@ptb.de

***Abstract*— We describe our experiment which evaluates frequency shifts due to collisions in a 1-D optical lattice clock with ^{88}Sr. The atoms in the lattice are probed on the $^1S_0$-$^3P_0$ transition which is highly forbidden but becomes weakly allowed by applying a static homogeneous magnetic field which mixes $^3P_1$ to the $^3P_0$ state. Using the method of interleaved stabilization, we have quantified the density dependent shift of the ^{88}Sr clock transition. By knowing the coefficient of the shift we can determine optimum conditions under which a 1-D lattice clock with ^{88}Sr can be operated with a fractional accuracy of 10^{-16}.**

I. Introduction

Optical transitions with millihertz linewidth have made lattice based clocks to perform better than the present microwave clocks [1]. The performance of optical lattice clocks paves way for a possible redefinition of the time unit 'second'. Bosonic and fermionic isotopes of strontium are being actively investigated as candidates for optical lattice clocks [2]–[5]. In case of a 1-D lattice clock based on the fermion ^{87}Sr, short range interactions would be more suppressed for identical particles at ultra-low temperatures due to the Pauli exclusion principle, but s-wave collisions are present for the boson ^{88}Sr. However, the ^{88}Sr isotope offers the advantage of higher natural abundance (82.58%) and a simpler laser cooling scheme compared to ^{87}Sr. Collisions in a ^{88}Sr lattice clock can be suppressed by using a three dimensional lattice having an occupancy of at most one atom per lattice site [4]. But such a 3-D lattice largely increases the complexity of the experimental setup. By studying the collisions in a 1-D lattice clock based on ^{88}Sr, we have characterized its performance and determine its operational limits. In a 1-D optical lattice clock based on ^{88}Sr, possible collision-induced effects are inelastic losses, broadening of the clock transition due to collisions and collision-induced frequency shift. The three effects are studied and reported in [8]. This paper concentrates on our experiment to determine the collision-induced frequency shift.

II. Experimental Procedure

A. Cooling and trapping of ^{88}Sr

The energy levels relevant to the scope of this paper are shown in Fig. 1. Cooling and trapping of ^{88}Sr takes place in two stages. The atoms coming out of an oven heated to 500°C

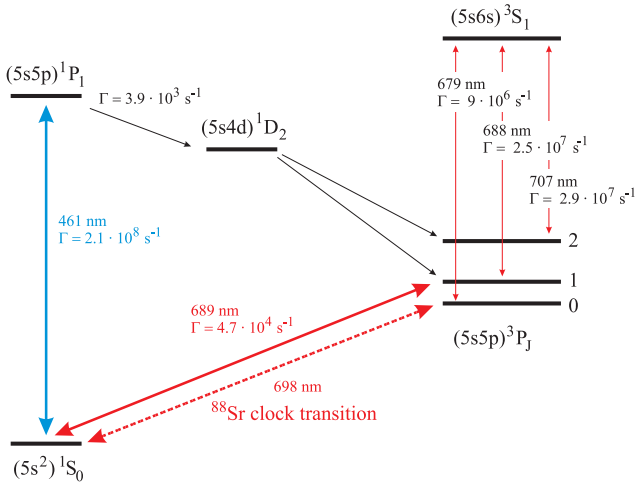

Fig. 1. Partial strontium energy level scheme. Γ denotes the spontaneous decay rate.

are slowed using a 38 cm long Zeeman slower. When they enter the vacuum chamber, atoms are deflected by an angle of 15° by a 2-D optical molasses. They travel a distance of 15 cm before being loaded into the first stage magneto optical trap (MOT). This first stage MOT is operated on the $^1S_0$-$^1P_1$ transition (FWHM = 32 MHz) at 461 nm. Total intensity of the cooling beams is 17 mW/cm^2 and the quadrupole field gradient is 18 mT/cm. With a typical loading time of 250 ms, the atoms are cooled down to 3 mK. The number of atoms in the $^1S_0$-$^1P_1$ MOT is 3×10^7 and can be increased by an order of magnitude by using the 679 nm and 707 nm repumping lasers (see Fig. 1). The second stage cooling operates on the $^1S_0$-$^3P_1$ (FWHM = 7.6 kHz) intercombination line at 689 nm. The laser used for this second stage cooling is frequency modulated at 50 kHz with a maximum frequency shift of 1.5 MHz from the detuning frequency to increase the capture velocity range. This frequency modulated stage lasts for 30 ms after which the modulation is turned off and the cooling laser is operated at single frequency for another 50 ms to cool around 1×10^7 atoms further below 4 μK. The total intensity of broadband stage and single frequency stage $^1S_0$-$^3P_1$ MOT beams are 8 μW/cm^2 and 180 μW/cm^2 and the quadrupole field gradient is 0.5 mT/cm. We determine atom number

978-1-4244-3510-4/09/$25.00 ©2009 IEEE

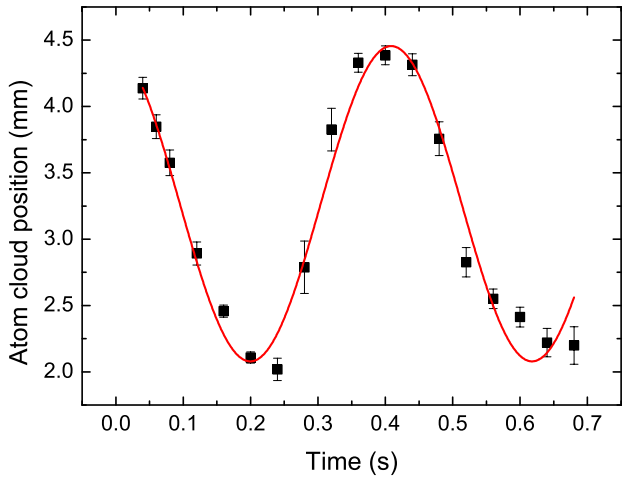

Fig. 2. Trap oscillations in axial direction excited by loading the atoms at a position away from the potential minimum of the dipole trap. The power of the dipole beam is 600 mW. Squares represent the measured position of the center of mass of the atoms in the dipole trap. The solid line is a sinusoidal fit to the data.

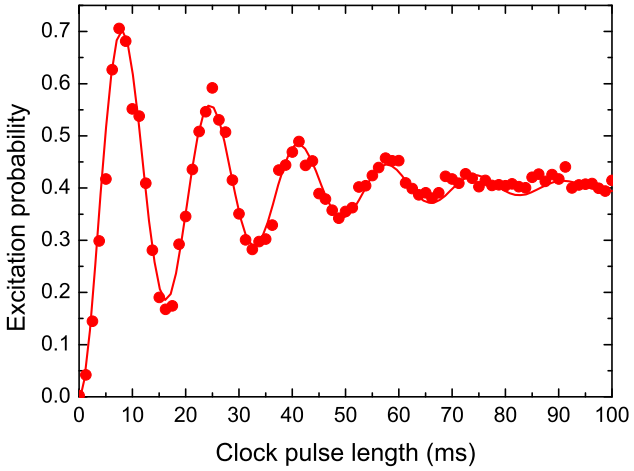

Fig. 3. Observed Rabi oscillations for 3 mT magnetic field and a clock laser intensity of 84 W/cm^2. The solid line is a fit of a damped Rabi oscillation.

and temperature of the atomic cloud by absorption images. Mechanical shutters are employed to block stray light.

The optical lattice laser is aligned horizontally and is overlapped with the atoms in the MOT during the whole cooling cycle. A standing wave is formed by retro-reflecting the beam. A Ti:Sapphire laser is used as lattice laser and is operated at the magic wavelength of 813 nm. In order to characterize the trap potential which is important to derive quantities like atomic densities, a dipole trap is formed by blocking the retro-reflected beam. The atoms are initially loaded in a position which is away from the potential minimum of the dipole trap in the axial direction. This is done by applying an offset magnetic field in addition to the quadrupole magnetic field used for the ^{1}S$_0$-^{3}P$_1$ MOT. The oscillation of the center of mass of the atomic cloud along the axial direction of the dipole trap is determined from absorption images. The position of the atomic cloud at different times of evolution is shown in Fig. 2. The angular frequency ω_z obtained from the fit is 15 rad·s^{-1} and the power of the dipole trap beam is 600 mW. By knowing these values, we have calculated the beam waist radius to be 34 μm.

We have used the same method to find the waist radius of the retro-reflected beam by loading the atoms in the reflected beam that is purposely not overlapped with the incoming beam. This method was also used to place the axial positions of the foci of the dipole trap beams at the position of the MOT and thus assure that the foci of both beams coincide. The maximum number of atoms trapped in the lattice after the second stage cooling is 3×10^6 which amounts up to 1000 atoms per lattice site.

The state mixing [7] of the ^{3}P$_1$ and ^{3}P$_0$ states necessary for the excitation on the clock transition is done by applying a homogeneous magnetic field. A π pulse is applied on the clock transition to excite the atoms. Details of the 698 nm laser system used to probe the ^{1}S$_0$-^{3}P$_0$ clock transition are given in Ref. [6]. The clock laser beam with a waist radius of 39 μm and a power of 2.0 mW is overlapped with the lattice through a dichroic mirror. We use a camera to check the extent of overlap between the lattice laser beam and the clock laser beam by placing a pellicle beamsplitter in the lattice laser path to deflect a part of the retro-reflected beam and the clock laser beam and observing the deflected beams at two or more points.

The excitation of the clock transition can be observed by two methods. The first method is by detecting the fluorescence of the remaining ground state ^{1}S$_0$ atoms by a 461 nm MOT phase. The second method involves pushing away the remaining ground state ^{1}S$_0$ atoms by using a resonant 461 nm beam immediately after the excitation to ^{3}P$_0$ state. The excited state atoms are brought back to the ground state by optically pumping them to the ^{3}S$_1$ state using 679 nm and 707 nm lasers and the fluorescence is detected using a 461 nm MOT phase. Observed Rabi oscillations with a homogeneous magnetic field of 3 mT and a clock laser intensity of 84 W/cm^2 are shown in Fig. 3. The fit for the Rabi oscillation shows 420 rad·s^{-1} Rabi frequency and a decay time of 25 ms due to coherence time of the clock laser.

B. Interleaved stabilization method

In order to measure the frequency shift of the clock transition due to collisions with other ^{88}Sr atoms, we use a technique in which the clock laser is locked to the ^{1}S$_0$-^{3}P$_0$ transition. The clock laser is detuned from the transition with frequency ν_0 by about $\pm\Delta/2$ where Δ is typically the transition linewidth (FWHM). This detuning is done by changing the frequency of the offset acousto-optical modulator (AOM) between clock laser and the cavity. We load the atoms into the lattice and excite the atoms to the ^{3}P$_0$ state by applying a π-pulse with a frequency $\nu_0+\Delta/2$. After the excitation pulse, we detect the excited state atoms. The cycle is repeated again with a frequency $\nu_0-\Delta/2$. A deviation ϵ of the mean clock laser frequency from ν_0 results in a non-zero difference between the

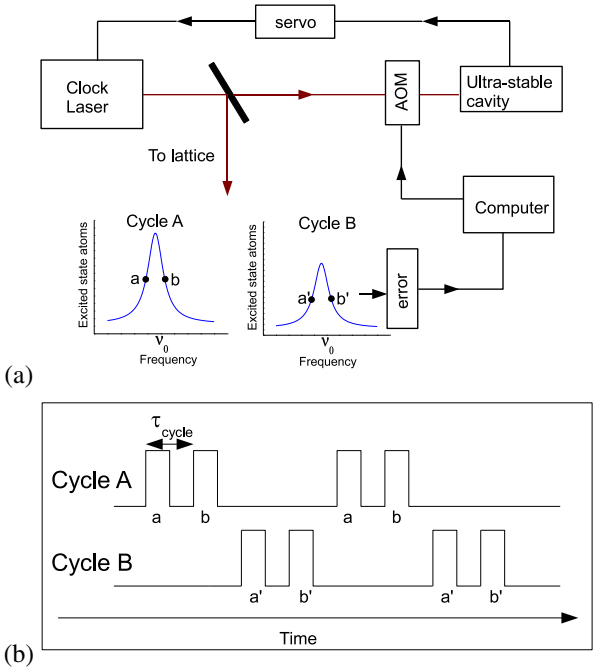

Fig. 4. Interleaved stabilization scheme. (a) Stabilization of the clock laser to the atoms. (b) Timing diagram for the interleaved stabilization with two different atom numbers in the lattice. A typical value of τ_{cycle} is 200 ms.

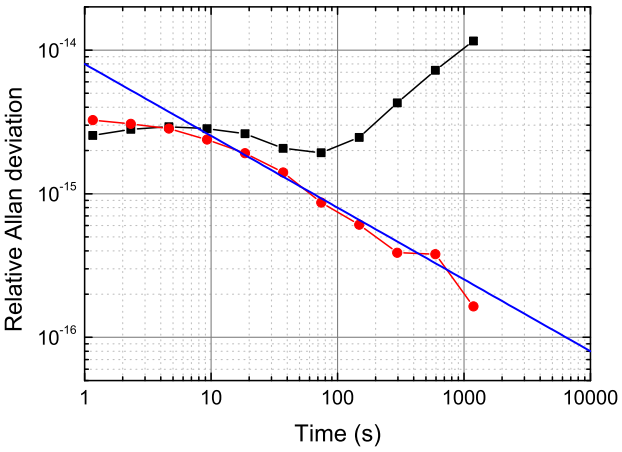

Fig. 5. Relative Allan deviations. Squares show the stability of the reference cavity with respect to the clock transition when a linear cavity drift is removed. Circles show the stability of the difference between cycles A and B with identical parameters for both cycles.

excited state atom numbers probed at $\nu_0 \pm \Delta/2$. To estimate ϵ, we assume that the clock transition has a Lorentzian profile. ϵ can be known by inserting it in the Lorentzian function and calculating the fluorescence signals S_1 and S_2 at $\nu_0 + \Delta/2$ and $\nu_0 - \Delta/2$, respectively. The relation between ϵ and the fluorescence signal is

$$\epsilon = \Delta \frac{S_2 - S_1}{2(S_2 + S_1)}. \quad (1)$$

The estimated deviation ϵ is fed back with an appropriate gain factor smaller than one to the clock laser-cavity offset AOM via the measurement program in order to keep the laser at the clock transition frequency. The gain factor introduces an effective time constant for the servo loop. We give the value of Δ as the input parameter in the measurement program for the correction. By using a detuning Δ different from FWHM, we can probe an ensemble of atoms with different excitation probability.

We use two different cycles named as cycle A and B in Fig. 4(a) to measure the frequency shift. These two cycles probe different number of atoms in the lattice. The atom number in the lattice is varied by changing the ^{1}S$_0$-^{1}P$_1$ MOT loading time in either cycle A or B. At the beginning of each cycle there is a darktime of 25 ms in which a resonant 461 nm beam is on. This darktime ensures that the remaining atoms from the previous cycle, if any, are pushed away and are not recaptured in the next cycle. Any recapture of atoms leads to systematic imbalance of the atom numbers in cycles A and B, and therefore to systematic frequency shifts.

Since the frequency drift of the laser due to change in the length of the stabilization cavity is roughly linear in time, we included a correction for this drift which was sent to the offset AOM between the clock laser and its reference cavity (Fig. 4(a)). The drift rate is automatically updated from the correction signal proportional to ϵ.

The timing diagram shown in Fig. 4(b) shows the interleaving of both cycles through which we can measure the frequency shift of the clock transition between two different number of atoms. By this method, we use the cavity as short term reference. This is possible because uncertainties from the limited predictability of the cavity drift on time scales of the cycle length are smaller than the shift to be measured. Random fluctuations can then be reduced by averaging.

III. Results

The experiment sequence was tested by having the same number of atoms in both cycles. Around 2×10^4 atoms were loaded into the lattice with power reduced to 150 mW by having a ^{1}S$_0$-^{1}P$_1$ MOT loading time of 16 ms. The cycle time τ_{cycle} was shortened to 200 ms by detecting the excited state atoms only. Squares in Fig. 5 show the relative stability of the clock laser reference cavity with respect to the clock transition frequency. The Allan deviation was calculated from the temporal evolution of the offset AOM frequency with a linear drift removed. The laser reached an optimum stability of 2×10^{-15} at $\tau \approx 70$ s and the stability decreased at longer times because of deviations from the linear cavity drift.

Circles in Fig. 5 show the stability of the difference between offset frequencies of sequential cycles A and B. We were able to reach a stability of 2×10^{-15} in $\tau = 18$ s. It shows white frequency noise behavior which scales as $1/\sqrt{\tau}$ indicated by the line. We could reach a fractional stability of 2×10^{-16} in $\tau = 1200$ s. The time constant for our locking system is 9 s which is consistent with the time at which the data deviates from the $1/\sqrt{\tau}$ line. We found that no systematic frequency

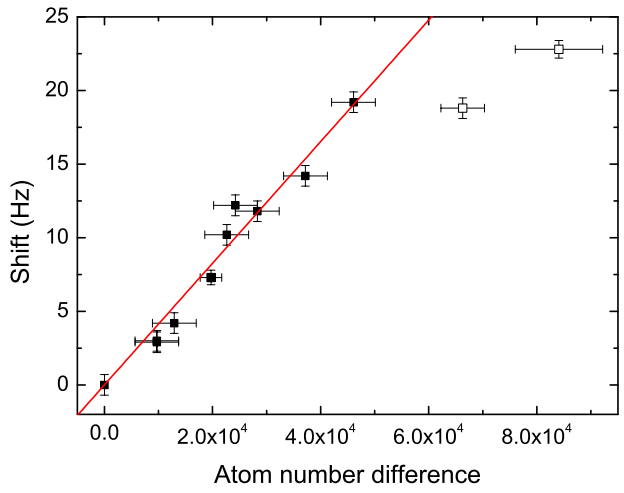

Fig. 6. Atom number dependent frequency shift of the ^{88}Sr clock transition.

shift occur at the level of few 10 mHz by taking the average of the difference of clock laser frequencies locked to the atoms.

Our observation of clock frequency shift with respect to atom number is shown in Fig. 6. To achieve a constant excitation probability even at high density [8], a 5 ms long π pulse is detuned such that the excitation probability is around 35% after the pulse. At low atom number, a linear dependence is observed but for high atom number a deviation from the linear behavior is seen. This deviation of frequency shift at high atom number could be due to change in dynamics during the excitation of the atoms because of losses and dephasing. We have calculated the coefficient for the frequency shift to be $(7.2 \pm 2.0) \times 10^{-17}$ Hz·m^3 excluding the open symbols shown in Fig. 6. The uncertainty in the shift coefficient is mainly due to density determination.

IV. Conclusion

We have described our experiment which evaluates frequency shifts due to collisions in a 1-D optical lattice clock with ^{88}Sr atoms. The technique of interleaved stabilization offers the advantage of measuring collisional shifts without a need for an external long term stable reference. From the linear fit in Fig. 6, the frequency shift as a function of atom number can be determined to better than 4%. Dependence of the frequency shift on the atom temperature was not observed when we varied the temperature between 2 μK and 4 μK. We therefore conclude that with 2×10^4 atoms in our present optical lattice collisions would not pose a limitation in a ^{88}Sr lattice clock if one wants to reach a relative accuracy of 10^{-16}.

Acknowledgment

The authors would like to thank Deutsche Forschungsgemeinschaft in SFB 407, the Centre of Quantum Engineering and Space-Time Research (QUEST), the European Community's ERA-NET-Plus Programme under Grant Agreement No. 217257, ESA, and DLR in the project Space Optical Clocks for their support.

References

[1] M. Boyd, A.D. Ludlow, S. Blatt, S.M. Foreman, T. Ido, T. Zelevinsky, and J. Ye, ^{87}Sr lattice clock with inaccuracy below 10^{-15}, *Phys. Rev. Lett.*, vol. 98, pages 083002-083005, 2007.

[2] G.K Campbell, A.D. Ludlow, S. Blatt et al., The absolute frequency of the ^{87}Sr optical clock transition, *Metrologia*, vol.45, pages 539-548, 2008.

[3] X. Baillard, M. Fouche, R.L. Targat et al., An optical lattice clock with spin-polarized ^{87}Sr atoms, *Eur. Phys. J.D.*, vol. 48, pages 11-17, 2008.

[4] T. Akatsuka, M. Takamoto and H. Katori, Optical lattice clocks with non-interacting bosons and fermions, *Nature Physics*, vol.4, pages 954-959, 2008.

[5] X. Baillard, M. Fouche, R.L. Targat et al., Accuracy evaluation of an optical lattice clock with bosonic atoms, *Optics Letters*, vol. 32, pages 1812-1814, 2007.

[6] T. Legero, C. Lisdat, J.S.R. Vellore Winfred et al., Interrogation laser for a strontium lattice clock, *IEEE Transactions on Instrumentation and Measurement*, vol. 58, pages 1252-1257, 2009.

[7] A.V. Taichenachev, V.I. Yudin, C.W. Oates et al., Magnetic field-induced spectroscopy of forbidden optical transitions with application to lattice-based optical atomic clocks, *Phys. Rev. Lett.*, vol.96, pages 083001-083004, 2006.

[8] Ch. Lisdat, J.S.R. Vellore Winfred, T. Middelmann, F. Riehle, and U. Sterr, Collisional losses, decoherence, and frequency shifts in optical lattice clocks with bosons, arXiv:0904.2515v2.